Journal of Energy Technologies and Policy
ISSN 2224-3232 (Paper) ISSN 2225-0573 (Online)
Vol.4, No.2, 2014

NO_x Emissions Prediction from a Turbulent Diffusion Flame

Akpan, Patrick [1] and Njiofor, Tobenna [2]
[1] Department of Mechanical Engineering, University of Nigeria, Nsukka
[2] Process Systems Engineering, Cranfield University, UK.
* E-mail of the corresponding author: Patrick.akpan@unn.edu.ng; +2348102475639

ABSTRACT

This work studies the finite volume technique of numerical discretisation by considering a transport process of diffusion. The case investigated is the prediction of NOx emissions from a turbulent diffusion flame arising from the combustion of methane in a cylindrical furnace. A finite volume-based method in a commercial CFD code (Ansys Fluent) was used.This simulation study was done in two and three dimensions. The assumption of constant specific heat resulted to over-prediction of NOx emissions from the combustion system while the use of variable mixture specific heat gave realistic results for the 2D and 3D simulations. The predicted average exit temperature and velocity of the flue gas were 1780 K and 3.12 m/s respectively for the 2D simulation, and 1800 K and 3.21 m/s respectively for the 3D simulation. The predicted mass fraction of NO pollutant (thermal and prompt) was 0.003311 and 0.004699 for the 2D and 3D simulations respectively.

Keywords: $k-\varepsilon$ turbulence model, NOx emission prediction, combustion modelling, Fluent, CFD, heat transfer, chemical reaction.

INTRODUCTION

In engineering processes, combustion nearly always takes place within a turbulent rather than a laminar flow field. This can be attributed to two reasons, the first being that turbulence increases the mixing process thereby enhancing combustion. The second reason is that combustion releases heat and thereby generates flow instability by buoyancy and gas expansion, which then enhances the transition to turbulence.
It is well known that combustion not only generates heat, that can be converted to power, but also produces pollutants such as CO2, oxides of nitrogen (NOx), soot, and unburnt hydrocarbons. Increasing stringent regulations are forcing manufacturers of automotives, power plants and industrial heating equipment to reduce pollutant emissions for the preservation of the environment. These emissions will be reduced mainly by improving the efficiency of the combustion process, thereby enhancing fuel economy. The key to such improvements will come from a thorough understanding of the combustion process, whether through experimental or CFD investigations, so as to be able to predict the flow pattern, temperature distribution, and species concentrations and emissions from the process.
This research is devoted to a CFD investigation of turbulent diffusion flames in gaseous combustion systems with special emphasis on methane combustion in a cylindrical furnace. The objective of this study is to understand key flow patterns and temperature distribution as well as predicting NOx emission from such systems.

CFD Modeling of NOx Emissions from Combustion

NOx emissions consist of mostly nitric oxide (NO), and to a less extent nitrogen dioxide (NO_2) and nitrous oxide (N_2O). The emission of NOx into the environment is partly responsible for acid rain and causes ozone layer depletion as well as photochemical smog. Hence NOx in that sense is an environmental pollutant. The prediction of NO emission entails solving a transport equation for NO concentration given in Eq.1:

$$\frac{\partial(\rho Y_{NO})}{\partial t}+\frac{\partial(\rho u_i Y_{NO})}{\partial x_i}=\frac{\partial}{\partial x_i}\left[\rho D\frac{\partial(\rho Y_{NO})}{\partial x_i}\right]+S_{NO} \quad (1)$$

Y_{NO} is the mass fraction of NO in the gas phase, D is the effective diffusion coefficient and S_{NO} is the source term. The NO transport equation is solved based on a given flow field and combustion solution (Fluent Inc., 2006a). As a result, an accurate combustion solution becomes a prerequisite for NO pollutant prediction. The source term Y_{NO} in Eq.1 depends on NO formation mechanism. In laminar flames, and at the molecular level within turbulent flames, NO formation can be attributed to four distinct chemical kinetics processes: thermal NO

formation, Prompt NO formation, fuel NO formation, and intermediate N_2O. Only the thermal and prompt NO formation mechanisms were considered in this study.

Thermal and Prompt NO Formation

Thermal NO Formation

The formation of thermal NO is determined by a set of highly temperature dependent chemical reactions known as the extended Zel'dovich mechanism (Foster et .al., 998). The principal reactions responsible for the formation of thermal NO from molecular nitrogen are given as follows:

$$O + N_2 \leftrightarrow N + NO \quad (2)$$

$$N + O_2 \leftrightarrow O + NO \quad (3)$$

A third reaction (Eq. 4) has also been shown to contribute to thermal NO formation, particularly at near-stoichiometric conditions and in fuel-rich mixtures:

$$N + OH \leftrightarrow H + NO \quad (4)$$

The net rate of formation of NO via the reversible reactions Eqns. (2)–(4) is given in Eq. 5.

$$\frac{d[NO]_T}{dt} = k_{f,1}[O][N_2] + k_{f,2}[N][O_2] + k_{f,3}[N][OH] - k_{r,1}[NO][N] - k_{r,2}[NO][O] - k_{r,3}[NO][H] \quad (5)$$

Where all concentrations have units of g mol/m^3 and $k_{f,1}$, $k_{f,2}$, $k_{f,3}$, $k_{r,1}$, $k_{r,2}$ and $k_{r,3}$. are the rate constants for the forward and reverse reactions determined from the following expressions (units of m^3/g mol s) proposed by Hanson and Salimian (1984):

$$k_{f,1} = 1.8 \times 10^8 e^{-\frac{38370}{T}}$$

$$k_{r,1} = 1.8 \times 10^7 e^{-\frac{425}{T}}$$

$$k_{f,2} = 1.8 \times 10^4 T e^{-\frac{4680}{T}}$$

$$k_{r,2} = 3.81 \times 10^3 T e^{-\frac{20820}{T}}$$

$$k_{f,3} = 7.1 \times 10^7 e^{-\frac{450}{T}}$$

$$k_{r,3} = 1.7 \times 10^8 e^{-\frac{24560}{T}} \quad (6)$$

In order to calculate the rates of formation of NO and N, the concentrations of O, H, and OH must be known. In most combustion processes (except in extremely fuel-rich combustion conditions) the quasi-steady assumption for [N] which states that the rate of consumption of free nitrogen atoms is equal to the rate of its formation holds. Under this assumption, the NO formation rate (in g mol/m^3 s) is given in Eq. 7.

$$\frac{d[NO]}{dt} = 2\,k_{f,1}[O][N_2]\frac{\left(1-\frac{k_{r,1}k_{r,2}[NO]^2}{k_{f,1}[N_2]k_{f,2}[O_2]}\right)}{\left(1+\frac{k_{r,1}[NO]}{k_{f,2}[O_2]+k_{f,3}[OH]}\right)} \qquad (7)$$

To solve Eq.7 the concentrations of O atoms, the free radical OH, and the stable species N2 and O2 must be determined at first. Zel'dovich suggested that the thermal NO formation mechanism can be separated from the main combustion process, by assuming equilibrium values of temperature, stable species, O atoms, and OH radicals (Fluent Inc., 2006a). However, radical concentrations (O atoms in particular) are observed to be more abundant than their equilibrium levels hence necessitating different approaches to determining them. Three approaches are used to calculate the O atom concentration in Eq.7: the equilibrium approach, the partial equilibrium approach, and the predicted O approach. Once the concentrations of O atoms, the free radical OH, and the stable species N2 and O2 are known, the thermal NO formation rate can be determined from Eq.7. In terms of the transport equation for NO, the NO source term due to thermal NO mechanisms is therefore calculated from Eq. 8.

$$S_{thermal,NO} = M_{w,NO}\frac{d[NO]}{dt} \qquad (8)$$

Where $M_{w,NO}$ is the molecular weight of NO (kg/g mol)

Prompt NO Formation

Prompt NO identified by Fenimore (1971) is most prevalent in rich flames. The actual formation process involves a complex series of chemical reactions and many possible intermediate species. The route that is accepted in the literature is given below (Fluent Inc., 2006a):

$$\begin{aligned} CH + N_2 &\leftrightarrow HCN + N \\ N + O_2 &\leftrightarrow NO + O \\ HCN + OH &\leftrightarrow CN + H_2O \\ CN + O_2 &\leftrightarrow NO + CO \end{aligned} \qquad (9)$$

The first reversible equation in Eq.9 is of primary important as studies by Scheferet. al.(1991) suggested that the majority of the NO at the flame base is prompt NO formed by the CH reaction. For most hydrocarbon fuels, the modified ***DeSoete model*** given in Eq.10 is used in determining the prompt NO formation rate (in g mol/m^3):

$$\frac{d[NO]}{dt} = f\,k'_{pr}[O_2]^a[N_2][FUEL]_\beta^{E'_a/RT} \qquad (10)$$

$$f = 4.75 + 0.0819\,n - 23.2\phi + 32\,\phi^2 - 12.2\phi^3 \qquad (11)$$

where a is the oxygen reaction order, f is a correction factor, and R is the universal gas constant. In the above equation,

$$k_{gr}' = 6.4 \times 10^6 (RT/p)^{a+1} \; ; \; E_a' = 303474.125 \; \frac{J}{g}\text{mol}$$

n is the number of carbon atoms per molecule for the hydrocarbon fuel, $\emptyset$ is theequivalence ratio, and *p* is the pressure.

MATERIALS AND METHOD

Problem Description

The problem considered here is the burning of pure methane (CH4) jet with coflowing air jet in a cylindrical combustor. The flame is a turbulent diffusion flame. The cylindrical combustor, of length and diameter 1.8 m and 0.45 m respectively, is shown in Figure 1. A small nozzle of diameter 0.01 m in the centre of the combustor introduces methane at a velocity of 80 m/s while ambient air also coaxially enters the furnace in a stream different from that of methane at 0.5 m/s. The overall equivalence ratio is approximately 0.76. From Yaws (2001), the density and dynamic viscosity of methane under the specified inlet condition are 0.664kg/m^3 and 110.72 x 10^{-7}Pa s respectively while the same properties for air are 1.199 kg/ m^{3}and 183.7 x 10^{-7}Pa s respectively. Hence, the Reynolds numbers of the air and methane jets are approximately 14360 and 47977 respectively. The combustor wall is kept at a temperature of 300 K. The combustor is assumed to be operating under steady state. It is further assumed that gravity effects are negligible from geometrical considerations, and that the high-speed methane jet expands initially with little interference from the combustor wall entraining and mixing with the low-speed air.For this study, the combustion process was modelled using a global one-step reaction rate assuming complete conversion of the fuel to CO2 and H2O with the chemical reaction represented by Eq. 13.

$$CH_4 + 2O_2 \leftrightarrow CO_2 + 2H_2O \qquad (13)$$

Two-dimensional (2D) and three-dimensional (3D) simulations were carried out for comparison of results.

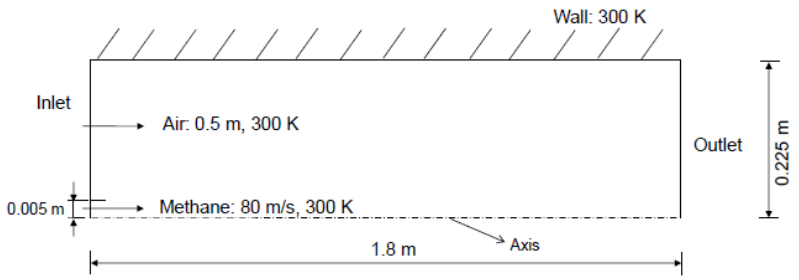

Figure 1 2D schematic diagram of the combustion of methane in a cylindrical combustor

Computational Details

Computational Domain

The 2D and 3D computational domains are shown in Figure 2 and Figure 3 respectively. Both grids were created in GAMBIT. The axisymmetric (two dimensional) model consists of a non-uniform structured grid of quadrilateral mesh elements. Because of the symmetry of the problem, only one quarter of the combustor was

modelled in three dimensions in order to reduce computational time. The 3D computational domain consists of an unstructured grid of hexahedral mesh elements.

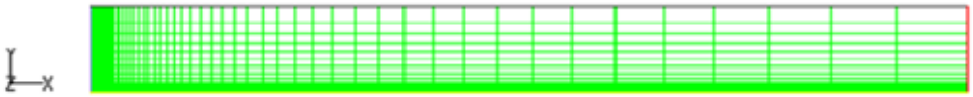

Figure 2 Combustor model for 2D simulation

Hexahedral mesh elements were used because the flow direction is parallel to the combustor wall. For the initial simulations, a total of 1891 nodes were used for the 2D grid while the 3D computational domain has 39266 nodes. The main reason for the non-uniformity of the grids is to capture the salient features of the combustion process.

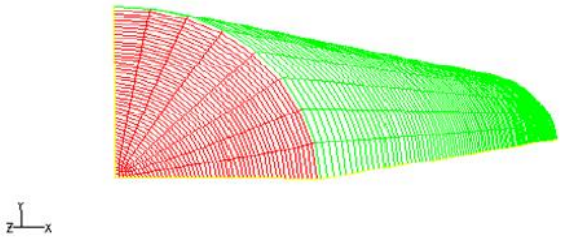

Figure 3 Combustor model for 3D simulation

Fluent Implementation

The NO transport equation is solved based on a given flow field and combustion solution thus obtaining a realistic combustion solution is essential to obtaining accurate NO pollutant prediction. The two and three-dimensional forms of the governing differential equations (continuity, momentum, turbulence, variables k(turbulent kinetic energyper unit mass)and ε (turbulent kinetic energy dissipation rate per unit mass), species transport) for steady flow were solved in Favre-averaged form by means of the Fluent pressure-based segregated solver. From experience well documented in Fluent Inc. (2006b) the standard $k-\varepsilon$ turbulence model was used for turbulence closure applying standard wall treatment as no swirl is involved in the combusting flow.

Furthermore, the species transport model with volumetric reactions available in Fluent was used for species modelling. The five volumetric species (CH_4, O_2, CO_2, H_2O, and N_2) involved in the chemical reactions were defined by means of the methane-air mixture material available in Fluent database (Fluent Inc., 2006a and Njiofor, 2009). The reaction represented by Eq.13 was defined in terms of the stoichiometric coefficients, formation enthalpies, and parameters that control the chemical reaction rate.

In addition, the reaction rate was calculated assuming that turbulent mixing is a rate-limiting process, with the turbulence-chemistry interaction modelled using the eddy-dissipation submodel. As density in a combusting flow is not a constant varying with temperature and composition, the incompressible ideal gas equation was used in calculating it. Also, the use of constant transport properties (except density) is acceptable as the flow is turbulent thus molecular transport properties will play a minor role compared to turbulent transport. Constant property assumption was initially used for the methane-air mixture (excluding density) after which the mixing-law (with the specific heats of the species computed using a piecewise polynomial function of temperature) was subsequently used to calculate the mixture specific heat. This was primarily done in order to determine the influence of constant specific heat input on combustion prediction. The prediction of the thermal and prompt NO pollutant based on Fluent model was undertaken after a converged solution of the flow field was obtained.

Boundary Conditions

As the quality of a CFD result is highly dependent on the specification of the appropriate boundary conditions, extra care was taken in specifying the correct boundary conditions for the computational model. Starting with conditions at the combustor inlet, a uniform velocity inlet boundary condition was implemented at the air and fuel inlets. At the combustor outlet, a constant pressure outlet boundary condition was applied since the exact details of the flow distribution were unknown. Also, the no-slip isothermal wall boundary condition was used at the wall of the combustor while an adiabatic wall boundary condition was applied at the walls of the fuel nozzle

since its heat transfer area is small. Finally, an axis boundary condition was implemented along the x - axis of the computational model in the 2D simulations while a symmetry boundary condition was implemented in the 3D case.

Discretization and Convergence Criteria

The convective fluxes contained in the governing equations were discretized using the first order upwind scheme while the central differencing scheme that is second order accurate was utilised to discretize the diffusive fluxes in the equations. Pressure-velocity coupling was achieved by means of the SIMPLE (Semi-Implicit Method for Pressure-Linked Equations) algorithm proposed originally by Patankar and Spalding (1972).

Model Verification and Validation

The law of conservation of mass was used to verify the accuracy of the obtained solution. For both the 2D and 3D simulations, the continuity equation must be satisfied at any two locations within the computational domain. The computed mass flow rate at the inlet and exit of the combustor were 0.0972112 kg/s and 0.0972135 kg/s respectively for the 2D simulation, and 0.0965878 kg/s and 0.0965873 kg/s respectively for the 3D simulation. Thus errors due to rounding off, iteration and discretization are very small as the requirement of the mass conservation law was met. However, the simulation results could not be validated with experimental data because of the absence of quality data at the time of this research. Most available data are on bluff body flames similar to the problem under study. However, comparison with previous works on bluff body flames in quiescent environment available in the literature show similar patterns between them.

RESULTS AND DISCUSSION

The results presented in this study are based on simulation with 6161 nodes forthe 2D simulations and 77966 nodes for 3D simulations. When a constant mixture specific heat of 1000 kJ/kg K was assumed thepeak temperatures attained for the 2D and 3D simulations were 3054 K and 3085 K respectively. These temperatures are clearly far greater than the adiabatic flame temperature for methane-air mixture at atmospheric conditions obtainable under these conditions. Thus the assumption of a constant mixture specific heat for the case being investigated may be the reason why the peak temperatures were over-predicted. Hence simulations with varying specific heats were considered more realistic for the problem under consideration and results for the 2D and 3D simulations are here presented.

Flow Field Development

The contours of velocity, temperature and mixtures specific heat capacity along the combustor length, for the resulting flow field in the 2D and 3D simulation are here presented.

Velocity contours

The contours of velocity magnitude revealed decreasing trend of velocity magnitude along the combustor length with maximum value occurring at the nozzle exit and the minimum value at exit from the combustor as shown in Figure 4 and Figure 5. Also, the contours of velocity magnitude plot in the 3D simulation has clearly defined (sharp) contour edges when compared to the 2D case because of high mesh resolution obtainable in 3D simulations that better captures turbulence effects.

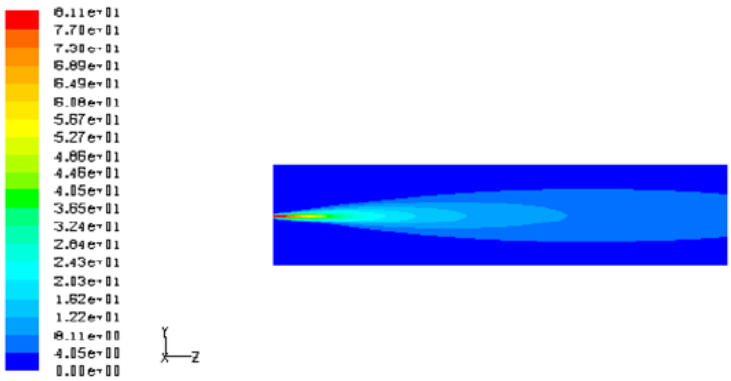

Figure 4 Contours of velocity magnitude for 3D simulation at Variable Cp

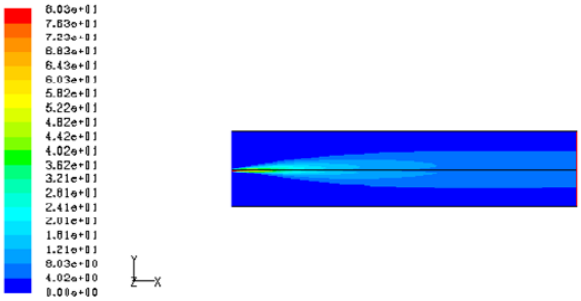

Figure 5 Contours of velocity magnitude for 2D simulation at Variable Cp

Temperature and Mixtures specific heat capacity (Cp) contours

The contour of temperature plot for the 2D and 3D simulations are shown in Figure 6 and Figure 7 respectively while the corresponding plots for the mixture specific heat are shown in Figure 8 and Figure 9 for the 2D and3D simulations respectively. It can be seen that the peak temperature dropped to 2277 K and 2309 K for the 2D and 3D simulations respectively as a result of the temperature and composition dependent specific heat. Also, the mixture specific heat is largest around the region of maximum concentration of CH_4 (near the fuel inlet) and

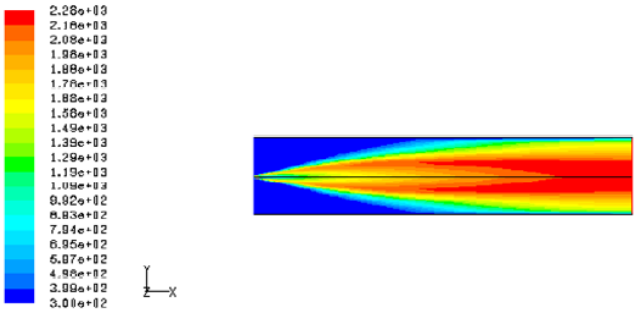

Figure 6 Contours of temperature for 2D simulation

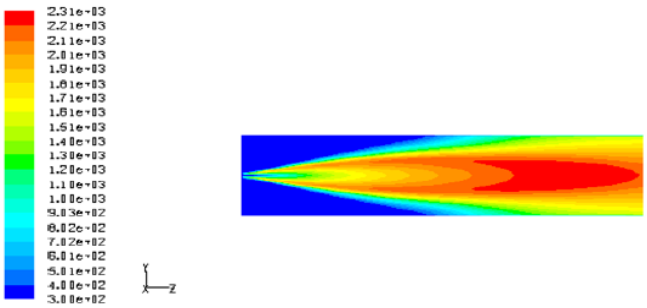

Figure 7 Contours of temperature for 3D simulation

where the temperature and composition product concentrations are large. The increase in heat capacity relative to the constant value used before significantly lowered the peak flame temperature. Comparison between the 2D and 3D plots showed that contour edges in the 3D simulation are again more highly defined than in the 2D simulation as a result of high mesh resolution obtainable in 3D simulation.

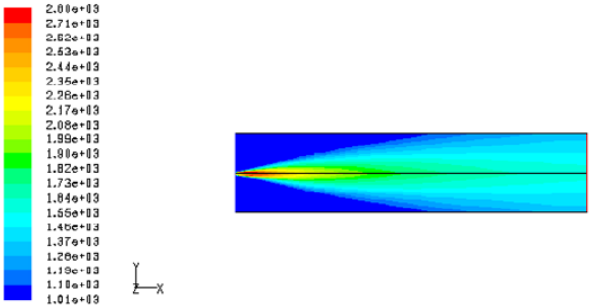

Figure 8 Contours of mixture specific heat for 2D simulation

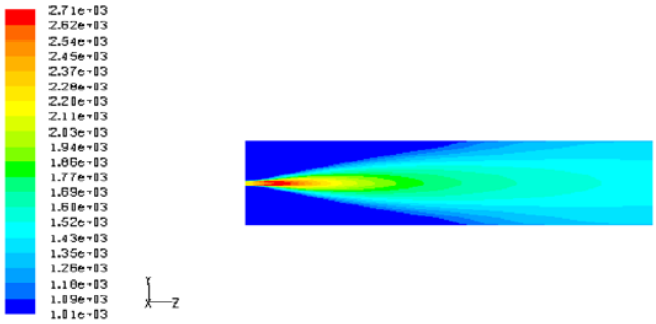

Figure 9 Contours of mixture specific heat for 2D simulation

NOx Mass Fraction Prediction

NO pollutant prediction was done in a post-processing mode using the NO_x model in Fluent with the flow field, temperature, and hydrocarbon combustion species concentrations haven been earlier determined. Hence, only the NO transport equation was computed. NO Prediction based on this mode is justifiedon the grounds of very low NO concentrations with negligible impact on theoverall prediction of the combustion process.

To calculate NO concentration, a time-averaged NO formation rate was computed at each node in the domain using the average flow-field information. Turbulence-chemistry interaction was determined using the normalised temperature probability density function (PDF) mode assuming 10-points beta PDF details of which can be found in the Fluent documentation (Fluent Inc., 2006a). The computations were done taken into account the contributions from thermal and prompt formation routes. The partial equilibrium assumption was used to calculate the [O] concentrations while contribution from [OH] was neglected with the assumption that its concentration is very small. The first order upwind and the central difference schemes were used to discretize the convective and diffusive fluxes respectively in the NO transport equation. Convergence was declared when the normalised residual of the NO transport equation became less than 10^{-6}.

The 2D and 3D predictions for the contours and radial profiles of mass fraction of NO species (both thermal and prompt) are shown in Figure 10 to Figure 13. It can be seen from the plots (see Figures 10 and 11) that peak concentration of NO species is located in the high temperature regions (combustor exit) where both O-atoms and N2 are available and conditions for chemical combination between them are favourable. This may be attributed to the high dependency of the rate of formation of thermal NO on temperature as evidenced by Eq.7. The radial profile of NO mass fraction plotted at 6 different locations along the combustor length (x/d or z/d = 5, 10, 30, 60, 100, and 180 where x or z is distance along the combustor length and d is nozzle diameter equal to 0.01m) plots shown in Figures 12 and 13 clearly shows that peak NO levels occurred at the exit of the combustor for both simulations.

Comparison between the 2D and 3D radial profile plots revealed that the mass fraction of NO species predicted is lower in 2D than in 3D simulation. This behaviour was as a result of the higher flame temperatures obtained in the 3D simulation. As the combustion process simulated in this work is lean, prompt NO production level is low when compared to the thermal NO production for both the constant and varying C_p mixtures (see Tables 1).

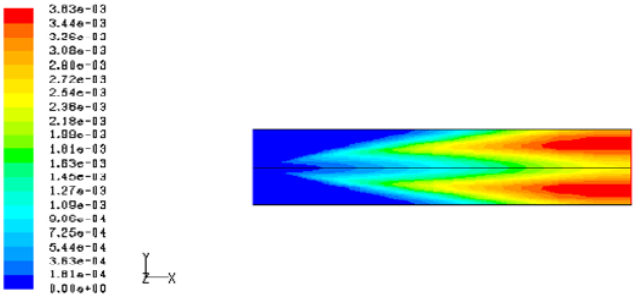

Figure 10 Contours of NO mass fraction for 2D simulation

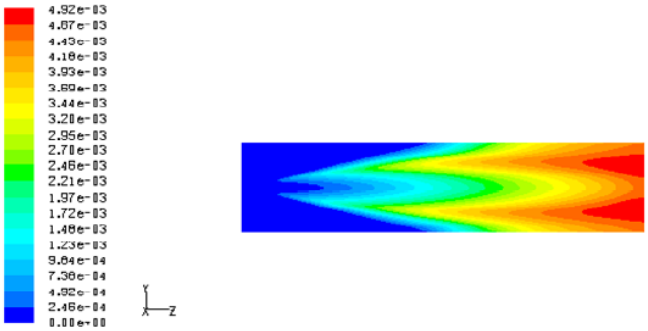

Figure 11 Contours of NO mass fraction for 3D simulation

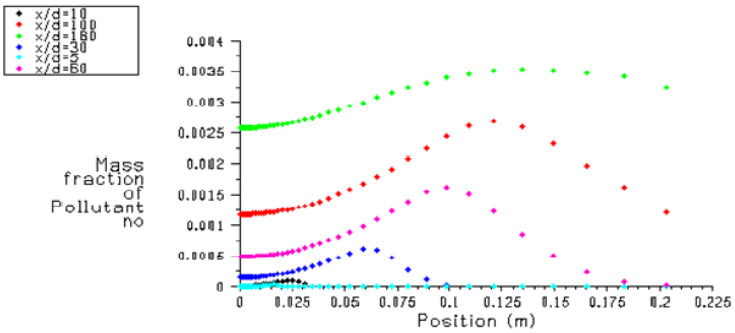

Figure 12 Radial profile plots of NO mass fraction for 2D simulation

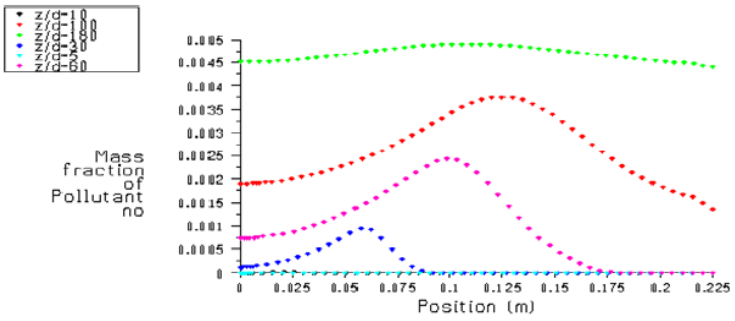

Figure 13 Radial profile plots of NO mass fraction for 2D simulation

Table 1 Combustion products exit condition

	Predicted Exit Variable	Constant Mixture Cp		Variable Mixture Cp	
		2D Simulation	3D simulation	2D Simulation	2D Simulation
1	Temperature (K)	2074	2207	1780	1800
2	Velocity (m/s)	3.62	3.94	3.12	3.21
3	CO_2 mass fraction	0.103939	0.114576	0.113039	0.115048
4	H_2O mass fraction	0.085095	0.093803	0.092545	0.094189
5	CH_4 mass fraction	0.003609	0.000378	0.001630	0.000115
6	O_2 mass fraction	0.069234	0.053703	0.055420	0.053017
7	N_2 mass fraction	0.738123	0.737540	0.737365	0.737630
8	NO mass fraction (thermal & Prompt)	0.022005	0.021687	0.003311	0.004699
9	NO mass fraction (Thermal only)	0.021992	0.021685	0.003273	0.004665
10	NO mass fraction (Prompt only)	0.005123	0.005060	0.000064	0.000073

In most combustion systems it is often desirable to know the condition of the flue gas before exit from the furnace for effective condition monitoring. The exit condition of the flue gas was determined using integral operators available in Fluent. The value of a given scalar quantity $\emptyset$at any required location can be evaluated using either the mass or area-weighted average surface integral operators defined as:

$$\text{Mass} - \text{weighted average}, \bar{\emptyset}_m = \frac{\int \emptyset \rho u . dA}{\int \rho u . dA} \quad (14)$$

$$\text{Area} - \text{weighted average}, \bar{\emptyset}_A = \frac{1}{A}\int \emptyset \, dA \quad (15)$$

Using Eqns. 14 and 15, the average exit condition of the flue gas was calculated for both the 2D and 3D simulations. The main results are summarized for simulations assuming constant and variable specific heat in Table 1. Comparison between the predicted average exit mass fraction of NO species for 2D and 3D simulations assuming constant specific heat was higher than the corresponding values obtained using variable specific heat. Hence NO emission was over-predicted in the constant specific heat simulations. The exit temperature and velocity were also over-predicted. Due to the higher temperature values attained in the 3D simulation, more NO pollutant emission was predicted in it than in the 2D simulation. However, the amount of NO pollutant predicted by both simulations is acceptable as they represent typical NO emission levels from turbulent diffusion flames.

CONCLUSION AND RECOMMENDATION

The finite volume-based commercial CFD software Fluent wasused to study the turbulent diffusion flame arising from the combustion of methane inside a cylindrical combustor in two and three dimensions with air as the oxidant. From the simulations, the important effect of the mixture specific heat on flame temperature was illustrated. It was seen that the assumption of a constant mixture specific heat resulted to a significant over-prediction of NOx emissions for the case investigated. Comparison made in Table 1 revealed that the average exit temperature and velocity were also over-predicted. The use of variable mixture specific heat resulted to realistic predictions in both the two and three-dimensional simulations. The predicted average exit temperature and velocity of the flue gases were 1780 K and 3.12 m/s for the 2D simulation and 1800 K and 3.21 m/s for the 3D case. The predicted mass fraction of both thermal and prompt NOx from the combustion system for the 2D and 3Dsimulations were 0.003311 and 0.004699 respectively. Further probe revealedthat NO production in this case study was dominated by the temperature sensitive thermal NOx mechanism.

Further improvement in the accuracy of prediction can be achieved by including the effects of intermediate species and radiation, both of which will reduce the predicted combustion temperatures. The single-step reaction mechanism used in this work does not account for the moderating effects of intermediate products of reaction, such as CO and H2. The effects of these species can be addressed using multiple-step reactions although more computational effort will be required for solving the additional species transport equations. Other models distinct in approach from the species transport model with volumetric reactions,such as the non-premixed combustion model can also be used to account for the effects of intermediate species at a reduced computational expense.

Radiation heat transfer tends to make the temperature distribution more uniform, thereby lowering the peak temperature hence the inclusion of radiation effects will have significant impacts on the simulation results.Modelling approach rather than the RANS-based approach is highly recommended.

Finally, the availability of experimental data for validating CFD results increases the credibility of CFD results and vice versa. It is therefore suggested that more experimental studies be undertaken in industrial combustion in order to produce high quality data for validation of CFD results.

REFERENCES

Fenimore, C. P. (1971). Formation of Nitric Oxide in premixed hydrocarbon flames. In: *Thirteenth International Symposium on Combustion,* TheCombustion Institute, 373 − 380.

Fluent Inc. (2006a).*Fluent 6.3 user guide documentation.* Fluent Inc., Lebanon.

Fluent Inc. (2006b).*Fluent 6.3 tutorial guide documentation.*Fluent Inc., Lebanon.

Foster T. J., Wilson C. W., Pourkashanian M. and Williams A. (2008) *Measurement and Prediction of NO and NO_2 Emissions from Aero Engines :*Paper presented at the RTO AVT Symposium on "Gas Turbine Engine Combustion, Emissions and Alternative Fuels", held in Lisbon, Portugal, 12-16 October 1998, and published in RTO MP-14.

Hanson, R. K. and Salimian, S. (1984). Survey of rate constants in H/N/O Systems. In: *Combustion chemistry*, edited by Gardiner, W. C. Springer, New York.

Njiofor, M. T. (2009). *Tool for numerical discretisation: finite Volume method for diffusion problems*. Cranfield University, UK. MSc Thesis Unpublished.

Patankar, S. V. and Spalding, D. B. (1972). A calculation procedure for heat, mass and momentum transfer in three-dimensional parabolic flows. *International J. Heat and Mass Transfer*, 15, 1787.

Schefer, R. W., Namazian, M. and Kelly, J. (1991). *Combustion Research Facility News,* vol. 3, No. 4. Sandia.

Yaws, C. L. (2001).*Matheson gas data book*, 7th Ed. McGraw-Hill, New York.

ACKNOWLEDGEMENT

The authors wish to thank the Nigerian government who through the Petroleum Technology Development Fund (PTDF) sponsored this research.

NOMENCLATURES

Symbols	Definition	Units
A	Area	[m^2];
a	Oxygen reaction order	[-]
c_p	Specific heat at constant pressure	[J/kg K]
D	Effective diffusion coefficient	[m^2/s]
f	Correction factor in the modified De Soete model	[-]
$(F/A)_{actual}$	Actual fuel/ air ration	[-]
$k_{f,1}, k_{f,2}, k_{f,3}$	Rate constants for the forward reactions in the Zel'dovich mechanism	[m^3/g mol s]
$k_{r,1}, k_{r,2}, k_{r,3}$	Rate constants for the reverse reactions in the Zel'dovich mechanism	[m^3/g mol s]
k'_{pr}	Rate constant for prompt NO formation in the De Soete model	[m^3/g mol s]
$M_{w,NO}$	Molecular weight of NO species	[Kg/g mol]
n	Number of carbon atoms per molecule for a hydrocarbon fuel	[-]
ϕ	Scalar variable	[-]
$\overline{\phi}_M$	Mass-weighted average of a scalar variable at a cell face	[-]
$\overline{\phi}_A$	Area-weighted average of a scalar variable at a cell face	[-]
ρ	Density	[kg/m^3]
R	Universal gas constant	[J/mol K]
$S_{thermal,NO}$	Source term of NO species due to thermal NOx Mechanism	[Kg/m3 s]
$S_{prompt,NO}$	Source term of NO species due to prompt NOx Mechanism	[Kg/m^3 s]
S_{NO}	Volumetric rate of production/destruction of NO species	[Kg/m^3 s]
T	Temperature	[K]
t	Time	[s]
$\mathbf{u}$	Velocity vector	[m/s]
u_i	Velocity components	[m/s]
x	displacement in x rectangular coordinate	[m]
Y_{NO}	Mass fraction of NO species	[-]